Parsing Pain Perception Between Nociceptive Representation and Magnitude Estimation

M. N. Baliki, P. Y. Geha and A. V. Apkarian

You might find this additional info useful...

Supplemental material for this article can be found at:
/content/suppl/2009/11/30/91100.2008.DC1.html

This article cites 58 articles, 17 of which can be accessed free at:
/content/101/2/875.full.html#ref-list-1

This article has been cited by 13 other HighWire hosted articles, the first 5 are:

Short-term meditation modulates brain activity of insight evoked with solution cue
Xiaoqian Ding, Yi-Yuan Tang, Chen Cao, Yuqin Deng, Yan Wang, Xiu Xin and Michael I. Posner
Soc Cogn Affect Neurosci, February 13, 2014; .
[Abstract] [Full Text] [PDF]

Shape shifting pain: chronification of back pain shifts brain representation from nociceptive to emotional circuits
Javeria A. Hashmi, Marwan N. Baliki, Lejian Huang, Alex T. Baria, Souraya Torbey, Kristina M. Hermann, Thomas J. Schnitzer and A. Vania Apkarian
Brain, September , 2013; 136 (9): 2751-2768.
[Abstract] [Full Text] [PDF]

Insular Cortex Mediates Increased Pain Tolerance in Yoga Practitioners
Chantal Villemure, Marta Ceko, Valerie A. Cotton and M. Catherine Bushnell
Cereb. Cortex, May 21, 2013; .
[Abstract] [Full Text] [PDF]

BOLD Responses in Somatosensory Cortices Better Reflect Heat Sensation than Pain
Eric A. Moulton, Gautam Pendse, Lino R. Becerra and David Borsook
J. Neurosci., April 25, 2012; 32 (17): 6024-6031.
[Abstract] [Full Text] [PDF]

Tracing Toothache Intensity in the Brain
M. Brügger, K. Lutz, B. Brönnimann, M.L. Meier, R. Luechinger, A. Barlow, L. Jäncke and D.A. Ettlin
J DENT RES, February , 2012; 91 (2): 156-160.
[Abstract] [Full Text] [PDF]

Updated information and services including high resolution figures, can be found at:
/content/101/2/875.full.html

Additional material and information about *Journal of Neurophysiology* can be found at:
http://www.the-aps.org/publications/jn

This information is current as of March 25, 2014.

Parsing Pain Perception Between Nociceptive Representation and Magnitude Estimation

M. N. Baliki,[1] P. Y. Geha,[1] and A. V. Apkarian[1,2,3]

[1]*Department of Physiology,* [2]*Department of Anesthesia, and* [3]*Department of Surgery, Northwestern University Feinberg School of Medicine, Chicago, Illinois*

Baliki MN, Geha PY, Apkarian AV. Parsing pain perception between nociceptive representation and magnitude estimation. *J Neurophysiol* 101: 875–887, 2009. First published December 10, 2008; doi:10.1152/jn.91100.2008. Assessing the size of objects rapidly and accurately clearly has survival value. A central multisensory module for subjective magnitude assessment is therefore highly likely, suggested by psychophysical studies, and proposed on theoretical grounds. Given that pain perception is fundamentally an assessment of stimulus intensity, it must necessarily engage such a central module. Accordingly, we compared functional magnetic resonance imaging (fMRI) activity of pain magnitude ratings to matched visual magnitude ratings in 14 subjects. We show that brain activations segregate into two groups, one preferentially activated for pain and another equally activated for both visual and pain magnitude ratings. The properties of regions in the first group were consistent with encoding nociception, whereas those in the second group with attention and task control. Insular cortex responses similarly segregated to a pain-specific area and an area (extending to the lateral prefrontal cortex) conjointly representing perceived magnitudes for pain and vision. These two insular areas were differentiated by their relationship to task variance, ability to encode perceived magnitudes for each stimulus epoch, temporal delay differences, and brain intrinsic functional connectivity. In a second group of subjects (*n* = 11) we contrasted diffusion tensor imaging–based white matter connectivity for these two insular areas and observed anatomical connectivity closely corresponding to the functional connectivity identified with fMRI. These results demonstrate that pain perception is due to the transformation of nociceptive representation into subjective magnitude assessment within the insula. Moreover, we argue that we have identified a multisensory cortical area for "how much" complementary and analogous to the "where" and "what" as described for central visual processing.

INTRODUCTION

Functional imaging studies in humans show that multiple brain regions are activated and modulated by nociceptive stimuli (Apkarian et al. 2005; Price 2000). However, brain areas specifically representing nociceptive properties remain elusive because many of the activations also reflect secondary processes, such as affective, cognitive, and anticipatory aspects of pain perception (Buchel et al. 2002; Coghill et al. 1999; Derbyshire et al. 1997; Rainville et al. 1997). For the pain sensory modality, intensity is its most salient and distinctive characteristic and yet the subjective magnitude assessment of painful stimuli (pain perception) is highly variable, because it is shaped by past experiences and current motivational states, and does not directly reflect incoming signals from primary sensory neurons (nociception) (Melzack and Katz 1999). Distinguishing nociception from magnitude perception in the brain has been explored only minimally (Apkarian et al. 1999). Here, by taking advantage of nonlinear stimulus–perception transformations for pain and the large intersubject variability in perceiving magnitude for constant painful stimuli, we differentiate brain areas that specifically encode painful stimuli from areas involved in assessing perceived magnitude of pain.

Magnitude estimation of pain intensity requires mapping the nociceptive signal to some sort of neural construct with numerosity representation (Piazza et al. 2007). Thus we speculate that this neural construct should involve brain regions that are not exclusive to pain perception but we also test the alternative—a magnitude-related brain region for the sense of pain. Little is known about cortical mechanisms underlying integrated magnitude estimation, although a number of candidate brain regions have been proposed (Piazza et al. 2007; Walsh 2003). We hypothesize that the transformation to pain perception involves brain areas integrating magnitudes across multiple sensory modalities.

Classical psychophysical studies have defined the properties of perceived magnitude. A mid-century seminal study by Miller (1956), and related observations made a century earlier by Weber in 1834 and by Fechner in 1860 (Fechner 1860/1966; Weber 1834/1978), showed that humans can identify one of five to seven intensities of different sensory stimuli, such as pitch, brightness, and saline concentration, with unique channel capacities for various sensory modalities. This evidence demonstrates the limited capacity of the brain for processing information, a notion that has been extensively pursued in relation to working memory (Cowan 2001). However, its implications for sensory information processing remain less developed. Miller's observations suggest a common central network underlying magnitude estimation that transforms sensory intensities into a percept of size. The transformation of the intensity of a physical stimulus into a perceptual magnitude estimation follows the power law proposed by Stevens [$\Psi = k\Phi^{\alpha}$, where Φ is stimulus intensity, Ψ is sensation magnitude, and α is an exponent, based directly on Weber's and Fechner's observations and theory, and casting these earlier results in a more solid mathematical framework (Stevens 1957)], where distinct power exponent values are observed for different sensory modalities (Gescheider 1997; Price 1988). Subsequent psychophysicists (Teghtsoonian 1971) theorized that distinct power laws imply a common magnitude eval-

uation system. Nonetheless, this theoretical construct has not been tested.

The capacity to code multimodal sensory information is undoubtedly limited by anatomical and physiological constraints. As such, a magnitude-assessing module in the human brain should exhibit extensive anatomical connectivity not only to sensory regions but also to higher cognitive brain areas. The insular cortex is one such brain region satisfying these requirements. It has wide connections with primary and secondary somatosensory areas, visual, auditory, and motor cortical areas, anterior cingulate cortex, basal ganglia (BG), amygdalae, several thalamic nuclei, and prefrontal cortex (Augustine 1996; Cipolloni and Pandya 1999; Mesulam and Mufson 1982). It also receives gustatory, olfactory, and visceral sensory inputs and is presumed to be the cortical region for primary taste representation and perception of flavor, by integrating these gustatory, olfactory, and somatosensory inputs (Critchley 2005; de Araujo et al. 2003; Hanamori et al. 1998; Rolls 2007). Furthermore, there is a large and accumulating literature indicating that the insula participates in pain perception. For example, a meta-analysis shows that in 48 functional magnetic resonance imaging (fMRI) studies of acute pain specifically examining insular activity, 45 concluded that it was activated for the pain condition (94% incidence) (Apkarian et al. 2005). In addition, the insula has also been shown to be activated for comparing numbers (Gobel et al. 2004), for determining stimulus magnitude by

ordering letters, numbers, and shapes (Fulbright et al. 2003), and seems to be part of a "core" task-set system, based on activity across ten different tasks (Dosenback et al. 2006).

In this study, we examine brain activity using fMRI in a single group of healthy subjects for assessing perceived magnitudes of thermal painful stimuli and the length of a visual bar. Subjects used a finger-span device to continuously rate and log the magnitude of their perceptions (Fig. 1A). The continuous ratings minimize brain activity associated with episodic memory and error detection. Our study is inspired by psychophysical cross-modality magnitude-matching experiments (Stevens 1957). Intensity to magnitude transformation for visual lengths is linear (exponent of power law $\alpha = 1.0$; Stevens 1957), whereas for contact thermal heat-induced pain the exponent for the stimulus–perception relationship is >3.0, resulting in a positively accelerating intensity to magnitude transformation (Nielsen et al. 2005). The latter implies that even if the two sensory modality tasks were equated at the stimulus level, they would result in distinct perceived magnitudes. Although earlier studies have matched perception for pain across subjects (Giesecke et al. 2004; Kwan et al. 2005; Lorenz et al. 2002), here we match perception between two senses, for magnitudes, within subjects. The rating pattern of perceived pain in each individual subject was used as input for that subject's visual bar length rating task. This enables a contrast between brain
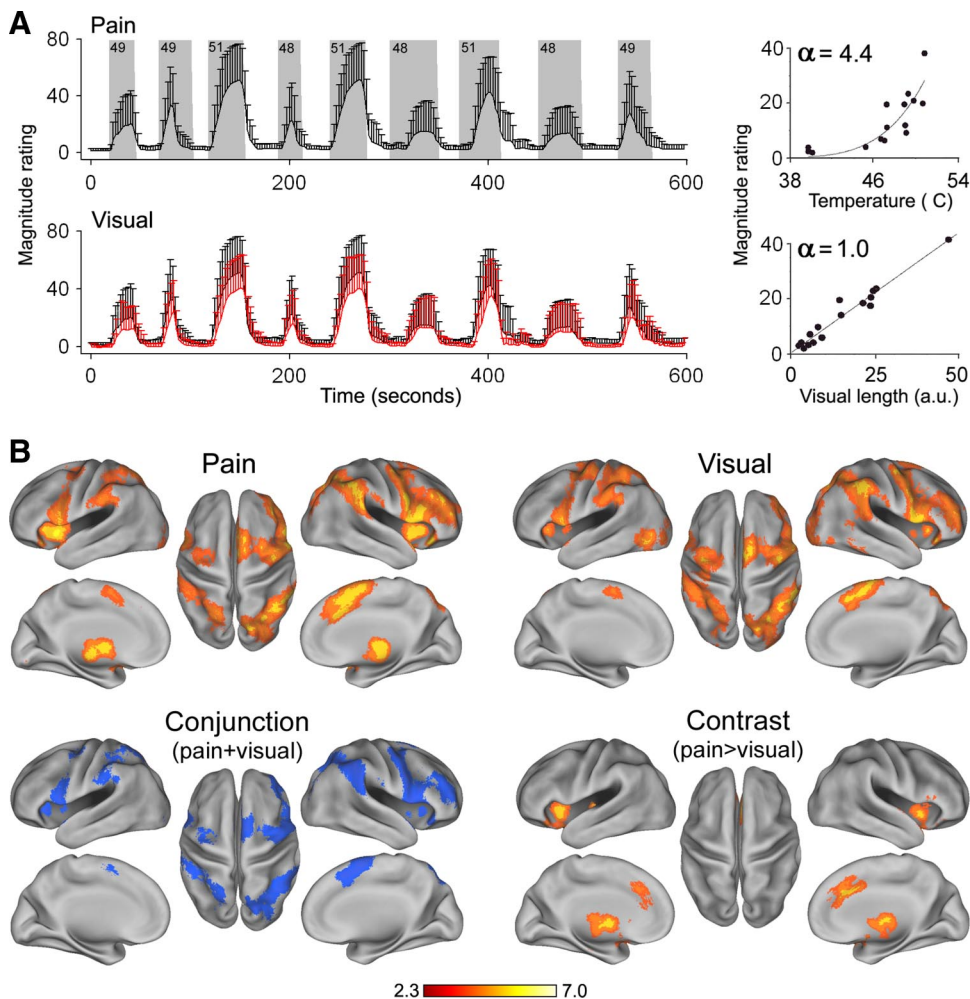

FIG. 1. Brain activity maps for pain- and visual-rating tasks. *A*, *top*: average pain ratings for painful heat. Gray areas delineate epochs and intensities (in degrees Celsius for the thermal stimuli). *Bottom*: average rating for the visual task. The *black trace* is the visual stimulus, obtained from the subject's pain ratings. The *red trace* corresponds to the subject's rating (bars are SD). Scatterplots show the relationship between stimulus intensity and perceived magnitudes and follows a power function with exponent of 4.4 for pain and 1.0 for visual ratings. *B*: random-effects analysis for pain- and visual-rating tasks. Many cortical areas were commonly activated. Bilateral thalamus and basal ganglia (BG) were active only during pain. The conjunction map between pain and visual rating is shown in blue and represents voxels that were commonly activated for both tasks and highlight many cortical regions, including portions of the insula. The contrast map shows regions significantly more active for pain rating and include bilateral thalamus and BG and parts of insula and middle portions of the anterior cingulate cortex (mACc). There were no regions that were more active for the visual rating.

activity for closely matched magnitude ratings but of distinct sensory modalities and valence (Fig. 2). We specifically compared brain responses to painful and visual stimuli because there is little ambiguity as to their disparate perceptions and assumed unique representations in the brain. Therefore discovering a common activation for both modalities would provide strong evidence for our hypotheses, which are as follows: *1*) properties of painful stimuli are captured by a network specialized in nociceptive representation; *2*) this information is acted on by a decision-making network, components of which are involved in assessing the magnitude of sensory inputs; *3*) the spatiotemporal transformation of information from the nociceptive network to the magnitude-related regions gives rise to perception of pain; and *4*) brain regions

estimating magnitude are multimodal and integrate information across the senses.

The results segregate the insula bilaterally into nociceptive-specific (noci-INS) and magnitude-related (mag-INS, which extended to the ventral premotor cortex) portions. The properties of these areas compared with each and with other activated regions were explored using multiple approaches to differentiate between sensory-specific representation and the more general magnitude encoding. Finally, in a second group of healthy subjects diffusion tensor imaging (DTI) was used to examine white matter tractography-based connectivity (Behrens et al. 2003a,b) of noci-INS and mag-INS with the rest of the brain, to test the hypothesis that these functionally distinct areas are a consequence of unique anatomical connectivity.
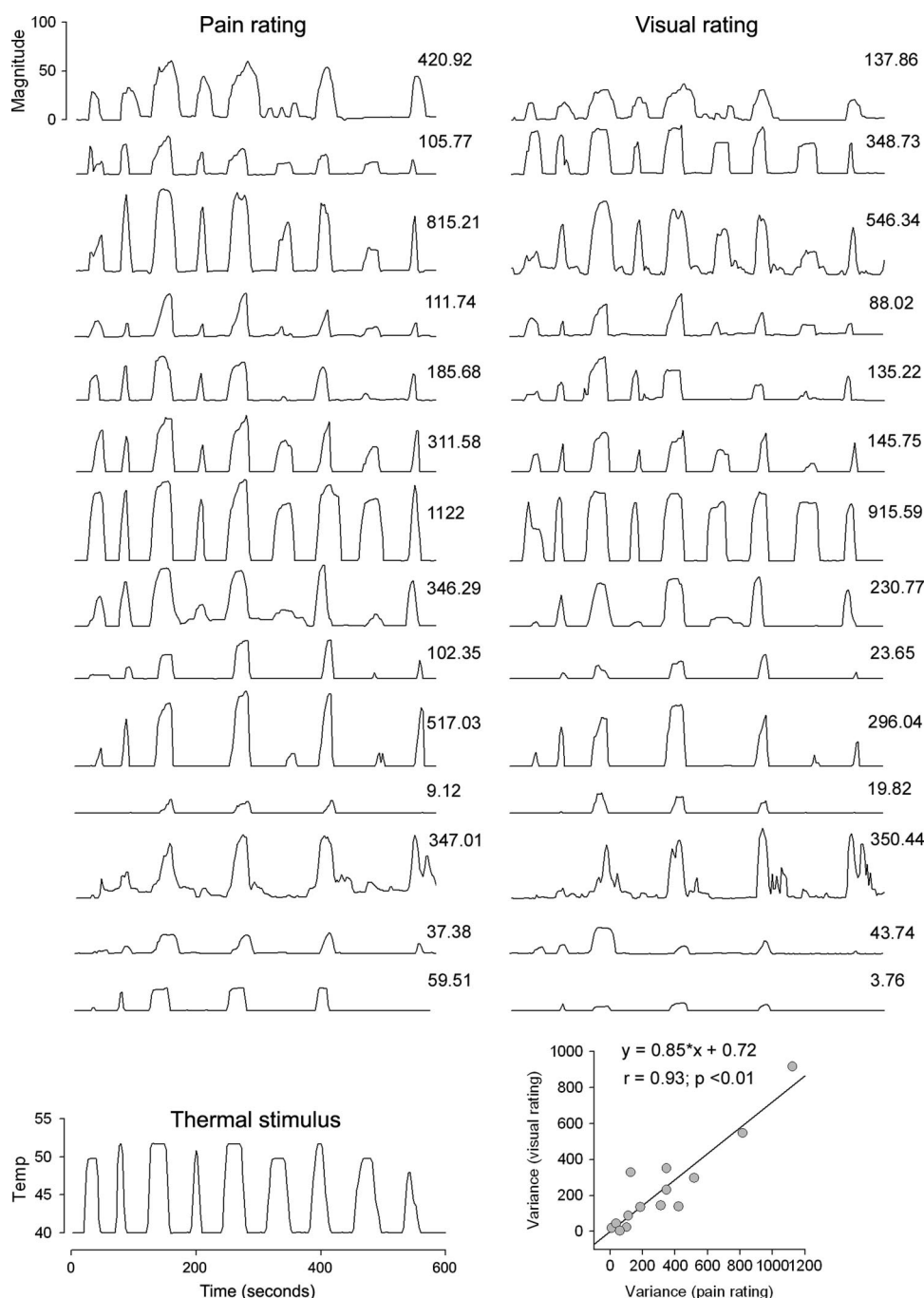
FIG. 2. Individual pain and visual magnitude ratings. *Left column* shows individual on-line subjective pain ratings for the 14 healthy subjects included in the study on a scale of 0–100, where 0 is no pain and 100 is maximum imaginable pain. *Right columns* show the corresponding visual on-line ratings using the same scale. Variances for the pain and visual tasks are shown next to the time courses. *Bottom left*: the time course of the thermal stimulus, monitored on the skin and averaged across all participants. *Bottom right*: the highly significant correlation between the variance for pain- and visual-rating tasks across 14 subjects, which is the stimulus–response relationship for the visual task.

METHODS

Participants

A total of 24 healthy subjects participated in the study. One group of subjects, who took part only in the fMRI study, included 7 healthy woman and 7 healthy men (age: 35.21 ± 11.48 yr; Beck Depression Inventory [BDI]: 4.38 ± 4.32; Beck Anxiety Inventory [BAI]: 5.22 ± 4.19); data are presented as means ± SD. A separate group of subjects were recruited for DTI study. These participants included 9 healthy woman and 3 healthy men (age: 33 ± 10.05 yr; BDI: 0.58 ± 1.16; BAI: 2.18 ± 3.57); data are presented as means ± SD. Participants were compensated financially for their time. All subjects were right-handed and all gave informed consent to procedures approved by the Northwestern University Institutional Review Board committee.

Pain-rating and visual-magnitude–rating tasks

Subjects were scanned while rating their pain in response to thermal stimuli applied to their back (pain-rating task) and rating the length of the bar in the absence of thermal stimulation (visual-rating task), using a finger-span device. Participants underwent an initial training phase prior to scanning, in which they learned to use the finger-span device to rate on-line changes in bar lengths., The finger-span device consisted of a potentiometer, the voltage of which was digitized and

time-stamped in reference to fMRI image acquisition and connected to a computer providing visual feedback (for further details see Apkarian et al. 2001; Baliki et al. 2006). A purpose-built, fMRI-compatible thermal stimulator delivered fast ramping (20°C/s) painful thermal stimuli (baseline 38°C; peak temperatures 47, 49, and 51°C) via a contact probe (1 × 1.5-cm peltier). Durations and intensities of thermal stimuli as well as interstimulus intervals were presented in a pseudorandom fashion. During a given functional imaging session, nine noxious thermal stimuli, ranging in duration from 10 to 40 s, were applied to the lower back at midline. Subjects were initially scanned once during acute thermal stimulation where they rated perceived magnitude of pain, resulting in 14 pain sessions. In the second functional scanning session, subjects rated the magnitude of the bar length, which unknown to them was varying in length with the pattern of their ratings of the thermal stimulus.

In the thermal task, subjects were provided with a visual feedback of their finger-span ratings, presented as a varying size bar with a scale indicating their rating on a 0–100 magnitude. The bar graph (in yellow color) was displayed on a black background of a computer monitor (occupying 80% of the screen) and was back-projected through a mirror set up within the scanner. In the visual task, the bar was controlled by the computer and the subject rated the size of the bar with the finger-span device. This design enables generation of magnitude ratings across the two sensory modalities that are matched
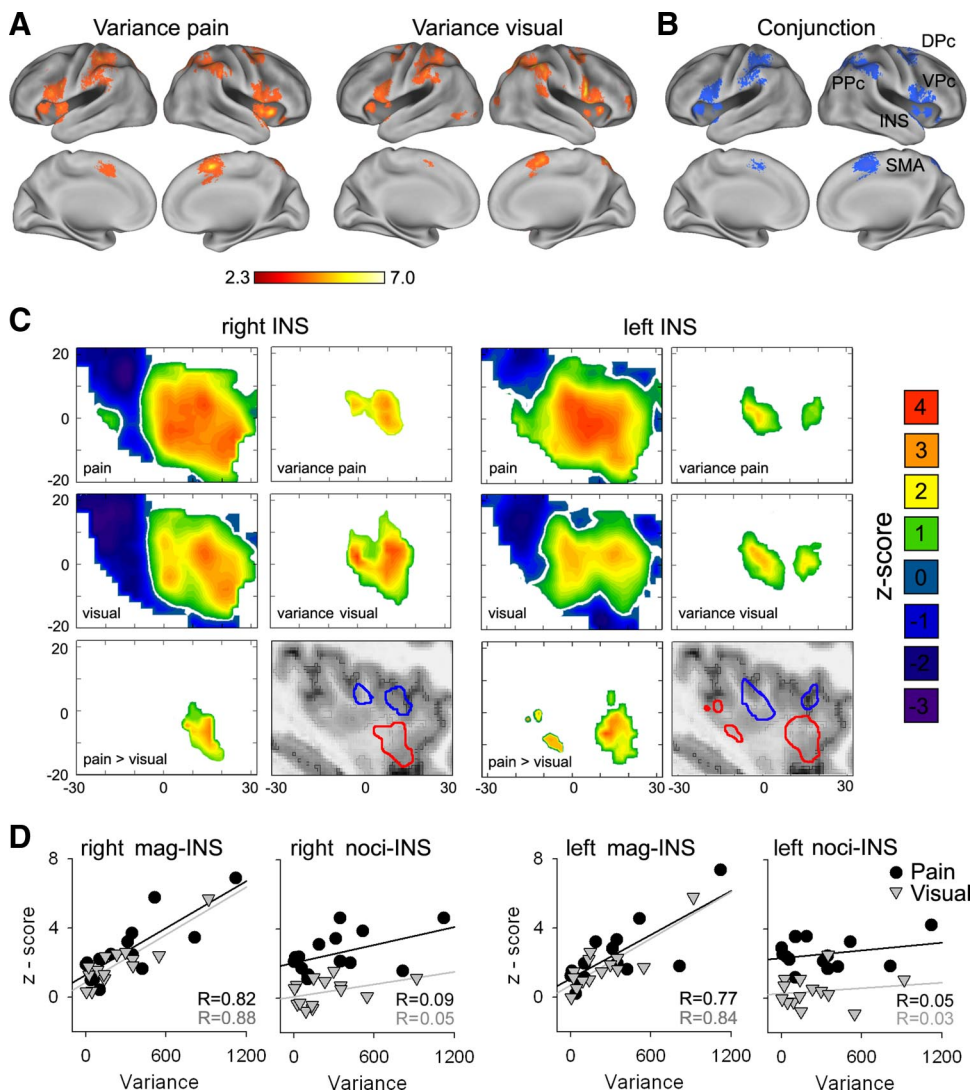

FIG. 3. Brain regions encoding variance of pain- and visual-rating tasks. *A*: whole brain covariate analysis between variance and brain activity for pain- and for visual-rating tasks. *B*: conjunction analyses for the pain and visual covariate maps; multiple cortical areas encoded variance in both tasks including bilateral ventral premotor cortex (VPc), posterior parietal cortex (PPc), insula, in addition to right dorsal premotor cortex (DPc) and supplementary motor area (SMA). *C*: topological maps for insular activity and variance encoding in pain- and visual-rating tasks. *Bottom right panels* show spatial dissociation for pain-specific activation (region that is significantly more active during pain than the visual-rating task, nociceptive-specific [noci-INS], red contour) and magnitude encoding areas (regions that are commonly activated and equally encode magnitudes during pain- and visual-rating tasks, magnitude-related [mag-INS], blue contour). *D*: scatterplots depict the relationship between brain activity from mag-INS and noci-INS (mean z-score) and variance for pain (circle) and visual (triangle) tasks.

within a subject but not across subjects (Supplemental Fig. S1),[1] where the visual inputs and finger movements are also matched for each subject.

fMRI data acquisition and analysis

Functional MR data were acquired with a 3-T Siemens Trio whole body scanner with echo-planar imaging (EPI) capability using the standard radio-frequency head coil. Multislice T2*-weighted echo-planar images were obtained with the following parameters: repetition time (TR) = 2.5 s; echo time (TE) = 30 ms; flip angle = 90°, slice thickness = 3 mm, in-plane resolution = 64 × 64. The 36 slices covered the whole brain from the cerebellum to the vertex. An average of 240 volumes were acquired per condition in all participants. A T1-weighted anatomical MRI image was also acquired for each subject using the following parameters: TR = 2.1 s, TE = 4.38 ms, flip angle = 8°, field of view = 220 mm, slice thickness = 1 mm, in-plane resolution = 0.86 × 0.86 mm^2, and number of sagittal slices = 160.

Image analysis, to reveal significant brain activity based on changes in blood oxygenated level–dependent (BOLD) signal, was performed on each subject's data using the Oxford Centre for Functional MRI of the Brain (FMRIB) Expert Analysis Tool (FEAT; Smith et al. 2004, http://www.fmrib.ox.ac.uk/fsl). The preprocessing of each subject's time series of fMRI volumes encompassed: skull extraction using a brain extraction tool (BET); slice time correction; motion correction; spatial smoothing using a Gaussian kernel of full-width half-maximum 5 mm; nonlinear high-pass temporal filtering (120 s); and subtraction of the mean of each voxel time course from that time course. The fMRI signal was then linearly modeled on a voxel-by-voxel basis using FMRIB's Improved Linear Model with local autocorrelation correction (Woolrich et al. 2001, 2004).

Pain and visual ratings were considered to generate a hemodynamic response described by the convolution of the corresponding vector with a generalized hemodynamic response function (gamma function: lag = 6 s, SD = 3 s). The pain- and visual-rating derivatives rectified and convolved with the hemodynamic function (modeling motor command) in addition to the six time series obtained from rigid head motion corrections were used as covariates of no interest, to remove residual variance due to head motion and minimize variance due to the motor task. The significance of the model fit to each voxel time series was calculated, yielding statistical parametric maps for each subject and condition. Average group statistical maps were generated using second-level random-effects group analysis. A cluster-based correction of the z-statistic images was performed and thresholded at z-scores >2.3. For each resulting cluster of spatially connected voxels surviving the z threshold, a cluster probability threshold of P = 0.01 was applied to the computed significance of that cluster, which corrects for multiple comparisons (Friston et al. 1995).

A two-sample paired t-test was used to compare visual- and pain-rating group average maps. A conjunction analysis was performed to determine spatial similarities in brain activity for the pain and visual-magnitude ratings. The conjunction map was generated by computing and multiplying the binary maps for average group statistical maps (voxels that were significantly activated were assigned a value of 1, otherwise 0) for pain and visual rating.

Task-variance encoding

Brain regions encoding task variance were identified using whole brain regression analysis in the FMRIB Software Library (FSL). First-level statistical maps were regressed with variance computed from the corresponding rating tasks for pain and visual maps. Average group statistical maps were generated using second-level random-effects group analysis for each task. Outcomes were then compared by contrast and conjunction analyses.

Regions of interest (ROIs) and BOLD responses

The ROIs were defined from the random effects analysis of pain − visual (pain-specific regions) or the pain + visual conjunction map (task-common regions) and delineated using automated anatomical labeling based on a macroscopic anatomical parcellation of the Montreal Neurological Institute MRI single-subject brain (Tzourio-Mazoyer et al. 2002). The ROIs were reverse-normalized and projected back into the nonnormalized individual brain space. The BOLD signal for the total trial duration was obtained by averaging the raw data for all voxels across a given ROI. The BOLD time course during stimulation epochs was measured first by calculating percentage BOLD change (deviation from the mean for voxels within the ROI), averaging across the nine stimulus repetitions for each phase, and averaging across all trials.

Magnitude encoding

For the purpose of examining the relation of magnitude ratings and brain activity, the hemodynamic response time curves were extracted from the ROIs and transformed into standard units by subtracting the mean of all points within the time series and dividing by its SD. The peak BOLD responses for each stimulation epoch and subject were extracted and correlated with the respective peak rating (irrespective of when that maximum rating occurred within the epoch) (see Fig. 4A).

Brain intrinsic correlational networks

Brain networks correlated to specific regional activity (seed) were identified using a well-validated method (see Baliki et al. 2008; Fox et al. 2005). Correlational network maps were produced by first extracting the BOLD time course from a seed region and, then, computing the correlation coefficient between its time course and the time variability of all other brain voxels, in first-level analysis in FSL. To combine results across subjects and compute statistical significance, z-score maps were generated for positive correlations using random-effects analysis corrected for multiple comparisons at a significance level P < 0.01. A two-sample paired t-test was used to compare connectivity maps across different seeds.

Surface-based mapping

This mapping was constructed using the PALS (Population-Average, Landmark- and Surface-based) average fiducial surface from 12 individual subjects as the atlas target (Van Essen 2005).

DTI data acquisition and analysis

We use DTI-based tractography to examine the relation between white matter connectivity and functional connectivity for brain areas that we observe to be functionally distinct. We recently described the procedure in detail (Geha et al. 2008). In 11 healthy subjects DTI images were acquired using spin-echo EPI in two acquisitions, 36 slices each, shifted by 2 mm in the z-direction to cover the whole brain with a total acquisition time of 11 min and 30 s. DTI parameters were: voxel size 1.7 × 1.7 × 2 mm in 9 subjects and 2 × 2 × 2 mm in the remaining 3 subjects; TR = 5 s, TE = 87 ms, flip angle = 90°, in-plane matrix resolution = 128 × 128. Diffusion was measured in 60 different noncollinear directions separated in time into seven groups by no-diffusion–weighted volumes for a total of eight no-diffusion–weighted volumes acquired for the purposes of registration and head motion correction.

---

[1] The online version of this article contains supplemental data.

Conjunction			Contrast		
ROI	Pain	Vis	ROI	Pain	Vis
R mag-INS	0.69**	0.65**	R noci-INS	0.32*	0.10
L mag-INS	0.52**	0.60**	L noci-INS	0.15	0.23
R VPc	0.59**	0.48**	R Thal	0.33*	0.06
L VPc	0.59**	0.42**	L Thal	0.11	0.11
R PP	0.08	0.13	R BG	0.12	0.01
L PP	0.09	0.11	L BG	0.26	0.14
DPc	0.19	0.14	R Amyg	0.19	0.11
SMA	0.21	0.10	L Amyg	0.09	0.15
			ACc	0.29*	0.12

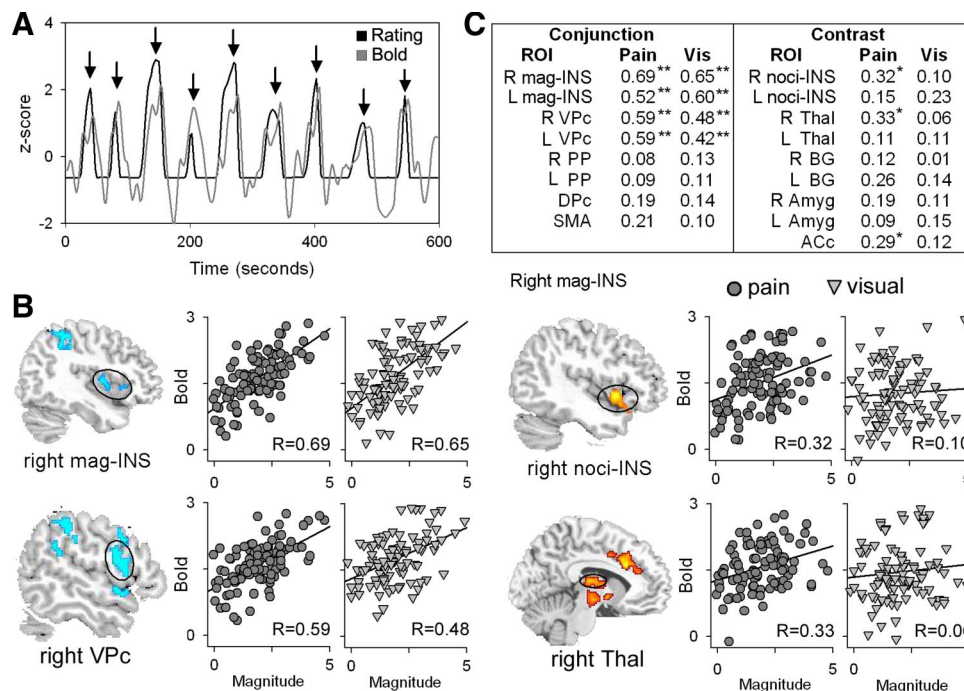FIG. 4. Brain regions encoding magnitude for visual and pain perceived magnitudes. *A*: example of blood oxygenated level–dependent (BOLD) signal and rating in standard units from one subject. Peak BOLD and rating were extracted for each stimulation epoch (indicated by arrows) and submitted for correlational analyses. *B*: correlation of BOLD with magnitude for 2 regions derived from the conjunction of variance-related map (blue) and contrast map (red). Scatterplots depict the degree of association between individuals' region of interest (ROI) signal and magnitude for pain (circles) and visual (triangles) stimuli. The ordinate represents functional magnetic resonance imaging (fMRI) signal and the abscissa represents the magnitude rating for each stimulus epoch for each participant. *C*: correlation strengths between rated magnitude and BOLD for pain and visual stimuli across task (conjunction) and pain-specific (contrast) regions. *$P < 0.01$; **$P < 0.001$. R, right; L, left.

Preprocessing of the DTI data included skull extraction using BET; correction for eddy currents and head motion was done by means of affine registration on the first no-diffusion–weighted volume of each subject. We performed tractography with the FSL Diffusion Toolbox in FSL 3.3 (Behrens et al. 2003b; Smith et al. 2004) by first running Markov-chain Monte Carlo sampling to build up distributions on the diffusion parameters at each voxel in the individual subject's space. Then we transformed the ROI (seed) into the space in which the DTI data were acquired per subject and from the seed masks we repetitively sampled the distribution on voxelwise principal diffusion directions, to generate a probabilistic sample from the distribution. Population probability maps of resulting clusters were generated by averaging the subject probability maps and applying a threshold of 100 of 5,000 samples.

We also defined target ROIs then generated probabilistic connectivity distributions from all voxels within the respective seed ROIs and quantified their probability of connection to each target. These probabilities were averaged over the seed ROI voxels. Differences in probabilistic connectivity between the seed ROIs to any target was computed using a nonparametric Mann–Whitney U test ($P < 0.05$).

RESULTS

Brain activity similarities and differences for pain and visual-magnitude ratings

Fourteen healthy subjects participated in this fMRI study. All were confident that they accurately performed both pain and visual ratings. These subjective ratings were used to identify brain activations associated with pain and visual ratings (see METHODS and Figs. 1A and 2) using the general linear model.

The pain-rating task was associated with increased brain activity in bilateral insula, left primary sensorimotor (S1/M1), and bilateral secondary somatosensory (S2) and posterior parietal (PPc), midtemporal (MT) cortices, dorsal and ventral premotor cortices (DPc and VPc), thalamus, putamen, caudate, and cerebellum, in addition to middle portions of the anterior cingulate cortex (mACc), supplementary motor area (SMA), and portions of the dorsolateral prefrontal cortex (DLPFc). Multiple studies report similar activations for acute pain (Apkarian et al. 2005; Price 2000). A visual-rating task exhibited increased activity in visual cortical areas as well as many areas observed for pain (Fig. 1B, Supplemental Fig. S1, Table 1).

To localize the brain regions commonly associated with rating of both painful- and visual-stimuli–driven magnitude ratings we performed a whole brain voxelwise conjunction analysis. Brain regions exhibiting significant activations for both rating tasks were restricted to the cortex and included bilateral insula, DPc, VPc, PPc, and MT, and midline activations in the mACc and SMA (Fig. 1B, Supplemental Fig. S2), suggesting that these regions might be commonly involved in both tasks. To identify brain regions more specifically related to either a pain- or visual-rating task, we carried out a paired t-test ($P < 0.01$). Brain regions showing greater activations for pain rating than for visual rating included regions in bilateral anterior insula, amygdalae, thalami, BG, and anterior portions of ACc as well as the ventral striatum (Fig. 1, Supplemental Fig. S2). There were no brain regions activated more for the visual task in contrast to the pain-rating task. The latter was expected for the visual cortical regions because the visual stimulus was matched between the two tasks. The distinction between brain regions specifically involved in pain, in contrast to the rating of either pain or visual magnitudes, closely replicates two recent studies where ratings for pain or touch stimuli—irrespective of whether performed simultaneously or immediately after stimulus—indicate a similar segregation between sensory-related areas and areas more related to the cognitive processing of sensory inputs (Kong et al. 2006; Schoedel et al. 2008).

Differentiating brain activity based on task variance

Given that the brain activity was fractionated to two minimally overlapping maps (the only overlap is in the insula), we

TABLE 1. *Peak foci for activation of pain and visual rating tasks and their contrast*

| Brain Region | Pain Rating | | Visual Rating | | Pain > Visual | |
| | Coordinates | | Coordinates | | Coordinates | |
	x, y, z	z-Score	x, y, z	z-Score	x, y, z	z-Score
R DLPFC (9/46)	40, 38, 30	5.99	48, 32, 30	5.91		
SMA (6)	−4, −6, 60	5.34	8, −6, 64	4.13		
Middle ACc (24)	2, 12, 40	6.47	6, 12, 38	3.47	8, 20, 30	3.86
L INS (13/14)	−38, 18, −4	6.12	−44, 6, 6	5.09	−42, −16, −10	3.93
R INS (13/14)	36, 24, −4	6.68	42, 10, 0	5.84	40, 12, −6	4.07
R S2	56, −36, 28	4.12	62, −36, 20	3.18		
L S2	−58, −32, 32	3.54	−66, −28, 18	3.44		
R PPc (40)	34, −50, 44	6.11	38, −54, 50	6.01		
L PPc (40)	−30, −54, 54	4.13	−32, −48, 50	5.32		
R VPc (4/6)	54, 12, 16	5.29	58, 10, 14	5.29		
L VPc (4/6)	−54, 6, 18	4.90	−50, 6, 16	4.14		
R FEF/DPc (4/6)	34, −4, 56	4.11	34, −10, 52	3.91		
L FEF/DPc (4/6)	−38, −8, 56	3.44	−38, −8, 50	4.08		
L MT+	−32, −74, 0	2.56	−52, −70, −4	6.03		
R MT+			54, −54, 10	4.12		
R TH	14, −20, 12	5.46			10, −14, −2	2.99
L TH	−14, −18, 4	4.24			−12, −20, −2	3.34
R putamen	22, 8, −4	5.31			28, 8, −6	2.70
L putamen	−24, −4, 6	4.91			−28, 0, 8	2.91
R Caudate	−18, 10, 14	2.76			−14, 18, 8	2.75
L Caudate	16, 10, 16	2.53			12, 16, 10	2.33
Anterior ACc (32)	4, 36, 20	4.48			6, 38, 22	2.59
R amygdala	22, 0, −18	2.84			20, 0, −18	2.32
L amygdala	−24, 0, −16	3.31			−20, −2, −20	3.58
Brain stem	2, −20, −12	3.92			−12, −20, −8	3.14
R cerebellum			38, −58, −38	3.40		
L cerebellum	−28, −64, −28	3.52	−30, −70, −36	3.25		

Brodmann Area shown in parentheses; x, y, z coordinates in millimeters. DLPFC, dorsolateral prefrontal cortex; SMA, supplementary motor area; ACc, anterior cingulated cortex; INS, insular cortex; S2, secondary somatosensory cortex; PPc, posterior parietal cortex; FEF, frontal eye field; MT+, middle temporal cortex; TH, thalamus; DPc, dorsal premotor cortex; VPc, ventral premotor cortex.

attempted to further segregate them along the dimension of the amount of information transmitted by each subject's ratings, as defined by Shannon and Weaver (1949). Classical psychophysical studies show that, within a given system, the amount of information is directly related to the variance of the performance (see Miller 1956). Therefore in this study, the amount of information perceived (and transmitted to the observer) during the pain and visual tasks was explored by the variance of the subjective ratings. The latter is a reflection of the tight correlation between pain ratings and the thermal stimulus, which implies that differences in variance are simply due to the individuals' relative sensitivity to the stimulus.

Within this framework, our experimental design provides several advantages in determining brain regions encoding perceived information. First, subjects provided continuous on-line ratings, which for the pain task were distinct from the stimulus time variability, and these ratings directly captured the subject-specific deviance of the perception for a constant stimulus. For the fixed thermal stimulus pattern (corresponding to a constant variance), participants showed magnitude ratings with a large range of variances (twofold difference in variance, between 9 and 1,122). Because the pain ratings with highest variances are the cases where the ratings better match the thermal stimulus time course (or variance), these values in most cases indicate a decrease in transmitted information regarding the thermal stimulus. Since the pain ratings were used as the input for the visual task and consistent with the linear stimulus–response transformation rule for visual bar lengths (Stevens 1957), we observe

a tight correlation between the visual input and corresponding perceived magnitude ratings where the variance again varies within a range matching that seen for the pain task (between 4 and 915). For the visual task, the range of variance is a reflection of the input variance and reflects mainly a preservation of input–output information (Fig. 2). Given that the variance for the visual- and pain-rating tasks are matched within subjects, this enables comparison of perceived information across two very distinct sensory modalities. Therefore we performed a whole brain covariate analysis of brain activity with variance of pain and variance of visual ratings across subjects to identify brain regions that reflect perceived information for each sensory modality. In both rating tasks, the amount of variance for magnitude rating exhibited a strong positive correlation with increased brain activity in bilateral PPc, insula, DPc, VPc, as well as SMA (Fig. 3A). It is worthwhile noting that none of the brain regions identified as specifically activated for pain showed an association with the variance for either the pain- or visual-magnitude–rating tasks. Moreover, the brain regions identified for each task are very similar and their conjunction (Fig. 3B) closely corresponds to the conjunction map we obtained based only on task-related activity. Potential artifacts and confounding factors that might contribute to the covariate analysis, such as performance proficiency and task demand, were investigated and discarded (for details see Supplemental Figs. S3 and S4). Thus these results allude to a common cortical network encoding the amount of variance (information perceived), for both sensory modalities,

with no overlap with the pain-specific regions. The brain regions identified correspond to a cortical network known to be involved in task control (for a wide range of conditions shown to be related to the start of a task, individual trials of tasks, and sustained activity across trials) (Dosenbach et al. 2006) and in spatial attention (including goal-directed responses and novel locations of objects) (Corbetta and Shulman 2002; Pihlajamaki et al. 2005). Although part of the insular cortex showed pain-specific activity, another portion of it was commonly active during both magnitude-rating tasks and was related to the variance of ratings in both tasks (Fig. 3C). This implies a functional dissociation whereby one insular subregion underlies nociceptive signaling and another seems involved in the more general task of perceiving magnitudes for both pain and vision.

We then studied directly the relationship of variance to brain activity by using region of interest (ROI) analyses. First, the ROIs within the insula were defined from the conjunction of the pain and visual covariate maps, distinguishing between nociceptive-specific (noci-INS) and magnitude-related (mag-INS) regions, and delineated using automated anatomical labeling based on a macroscopic anatomical parcellation of a single-subject brain (Tzourio-Mazoyer et al. 2002). Next the ROIs (mag-INS and noci-INS) were projected into individual subject space and the activity within the ROIs (mean z value across all ROI voxels) was computed. Figure 3C shows the association between activity in the two subregions of the insula and variance for the pain- and visual-magnitude–rating tasks across subjects. Consistent with the preceding results, bilateral mag-INS showed significant correlations with variance for both tasks ($P < 0.001$). By contrast, although noci-INS showed higher activity for pain than that for visual rating, it did not correlate with the variance of either task. Similar to mag-INS responses, bilateral VPc, PPc, and right DPc and SMA showed strong significant correlations with variance for both tasks, based on ROI analysis (Supplemental Fig. S5). Therefore the ROI analysis corroborates the distinction not only between mag-INS and noci-INS but also for the brain regions identified to be involved in rating perceived magnitudes, regarding representation of the variance of perceived magnitudes.

Coding for perceived magnitudes

The results so far suggest that these sensory-magnitude–rating tasks involve two distinct functional constituents. The first appears to be associated with rating performance, is correlated with the amount of information perceived by the subject, and is autonomous of sensory modality. The second appears to be pain modality specific and does not account for the variability in perception. It still remains unclear, however, which brain regions mediate the transformation of stimulus parameters into perceived magnitudes. One possibility is that it is mediated by early sensory-specific areas, alternatively by higher associative regions that are downstream within the processing organization (de Lafuente and Romo 2006) and are related to the variance of the ratings. Moreover, higher brain regions may encode variance by reflecting temporal properties of the tasks with or without relating this information with the magnitudes reported for each modality and each stimulus epoch. To distinguish between these options, we performed the ROI analysis examining noci-INS and other pain-specific re-

gions (derived from the pain − visual contrast map) and mag-INS and other variance-encoding brain areas. For each subject and ROI, the peak BOLD and its corresponding rating were extracted for each stimulation epoch and submitted to a correlational analysis (Fig. 4A; see METHODS for details). If a brain region encodes the perceived magnitude of a stimulus, we expect the extent of BOLD response in that region to be associated with each subjective magnitude rating of pain and/or visual stimuli. Results are shown in Fig. 4. Within brain regions reflecting task variance, bilateral mag-INS showed the best correlation with rated magnitudes for both pain and visual stimuli (right mag-INS, $r = 0.69$, $P < 0.01$ for pain, $r = 0.65$, $P < 0.01$ for visual; left mag-INS, $r = 0.52$, $P < 0.01$ for pain, $r = 0.60$, $P < 0.01$ for visual). Additionally, perceived magnitudes correlated with bilateral VPc activity ($P < 0.01$ for pain and for visual ratings), a region just lateral and contiguous with mag-INS. In contrast, bilateral PPc, DPc, and SMA, which showed significant correlations with task variance, were not correlated to perceived magnitude in either task (Fig. 4C).

Brain areas specifically activated for pain, including bilateral thalamus, BG, amygdalae, and anterior cingulate exhibited weaker correlations with magnitude during the pain-rating task, of which only right noci-INS ($r = 0.32$, $P < 0.05$), right thalamus ($r = 0.33$, $P < 0.05$), and ACc ($r = 0.29$, $P < 0.05$) were significant. Consistent with the above-cited results, pain-specific regions showed no significant magnitude encoding for the visual task (Fig. 4C). These results show that within brain regions reflecting task variance only mag-INS and VPc encode perceived magnitudes for both pain and visual stimuli. Additionally, for the pain-rating task, modality-specific brain regions were also related to perceived magnitude, albeit with weaker correlations. Therefore mag-INS and VPc seem seminal in sensory magnitude integration. Moreover, given that the relationship between perceived pain magnitudes and brain activity was highest in mag-INS and VPc, this must be a consequence of integration of information from multiple pain-specific regions, each of which shows a poorer correlation to perceived pain magnitudes.

Stimulus and perception relationships for the pain-rating task

In the pain task, stimulus and perception had distinct temporal patters. This enabled investigation of the spatiotemporal processing stages involved in the transformation of the stimulus into the perception of magnitude, by deriving BOLD parameters that assess the degree of association of brain regions with either the painful stimulus or the magnitude ratings. This method is borrowed from a recent study in monkeys, which showed a gradual buildup of single neuronal activity across multiple brain regions during the transformation of sensory information into a judgment (de Lafuente and Romo 2006). The features of our task design render this analysis possible for the pain-rating task because the stimulus and rating exhibit distinct peak latencies, with the ratings lagging behind the stimulus by an average of 7.5 s (Figs. 1A and 5A). The time course of the BOLD response for different ROIs was measured first by calculating percentage BOLD change (deviation from the mean for voxels within the ROI), averaging across the stimulus repetitions, and averaging across trials (see METHODS). The average time courses of the stimulus, pain ratings (both

convolved with hemodynamic response function), and BOLD signals for pain-specific and variance-dependent ROIs (see earlier text) were compared (Fig. 5A). Consistent with the aforementioned observations, the BOLD signal from the noci-INS and thalamus, nociceptive-specific regions, exhibited peak latencies and time courses similar to the stimulus. Brain regions that were equally activated for both pain- and visual-rating tasks and were variance dependent (i.e., right mag-INS, VPc, and PPc), on the other hand, exhibited BOLD responses with time course properties and peak latency responses comparable to those of perceived magnitudes.

Individual subject peak latency of BOLD response from the start of the stimulus, as well as the extent of correlation of the BOLD response to the stimulus in contrast to the ratings, indicated segregation of noci-INS and mag-INS within this two-dimensional space (Fig. 5B, top). Group average peak latencies and stimulus–perception correlation differences across the ROIs examined indicated that the ACc and amygdala exhibited the earliest responses (which on average preceded the stimulus peak), followed by thalamic and BG activity that showed the best relationship with the stimulus. Similarly to thalamic and BG responses, noci-INS showed better association with the stimulus and an early peak. On the other hand, mag-INS, VPc, and PPc showed more delayed peak latencies and the highest association with rating of perceived magnitudes (Fig. 5B, bottom). These results indicate that brain regions with longer latencies (more downstream in the processing stages) were better associated with the subjects' perception and that the insula plays an important role in the integration and transformation of sensory information in perceiving magnitude because noci-INS and mag-INS again segregate along these lines.

Functional and anatomical connectivity for subregions of insula

Multiple lines of evidence in the preceding sections indicate two functionally distinct subdivisions within the insula. Thus we examined brain functional connectivity and anatomical connectivity for these two regions (left mag-INS and noci-INS). The functional networks were generated by correlating the BOLD time courses from each of these regions with all other voxels in the brain for each subject and averaged across all subjects using random-effects analysis (z-score >2.3) (Fig. 6A). Brain areas with activity correlated with noci-INS and mag-INS were distinct and nonoverlapping. The mag-INS activity was correlated only with cortical areas and dominated by regions that captured task variance, including bilateral PPC, VPc, DPc, and SMA. In contrast, noci-INS had an extensive subcortical connectivity pattern and showed significant positive correlations with pain-specific regions, including bilateral thalamus, BG, and amygdalae in addition to anterior portions of the ACc and ventral striatum. The distinct connectivity patterns were significantly different (Supplemental Fig. S6).

Diffusion tensor magnetic resonance imaging (DTI) coupled with probabilistic tractography takes advantage of water diffusion along axons and allows the study of the structural connectivity of the white matter (Alexander et al. 2007; Beaulieu 2002). In a separate group of 11 healthy subjects we used DTI probabilistic tractography to test the notion that mag-INS and noci-INS have distinct white matter connectivities. Consistent with the functional segregation, the two subdivisions of the insula exhibited differential water-diffusion–based white matter connectivities. Seed ROIs for probabilistic maps were defined as a $5 \times 5 \times 5$-mm cube around the centers for mag-INS ($x = -44$, $y = 0$, $z = 4$) and noci-INS ($x = -36$, $y = 18$, $z = -4$). Mean probabilistic maps of white matter tracts for left mag-INS and noci-INS were distinct (Fig. 6B). White matter tracks from noci-INS traversed to the ipsilateral thalamus, striatum, basal ganglion, amygdala, and temporal gyrus. Tracks from mag-INS, on the other hand, were localized to the cortex and extended to S2, primary motor, and somatosensory regions and PPc. We also quantified, using probabilistic tractography, connections from noci-INS and mag-INS (using the same seed coordinates used earlier) to specific
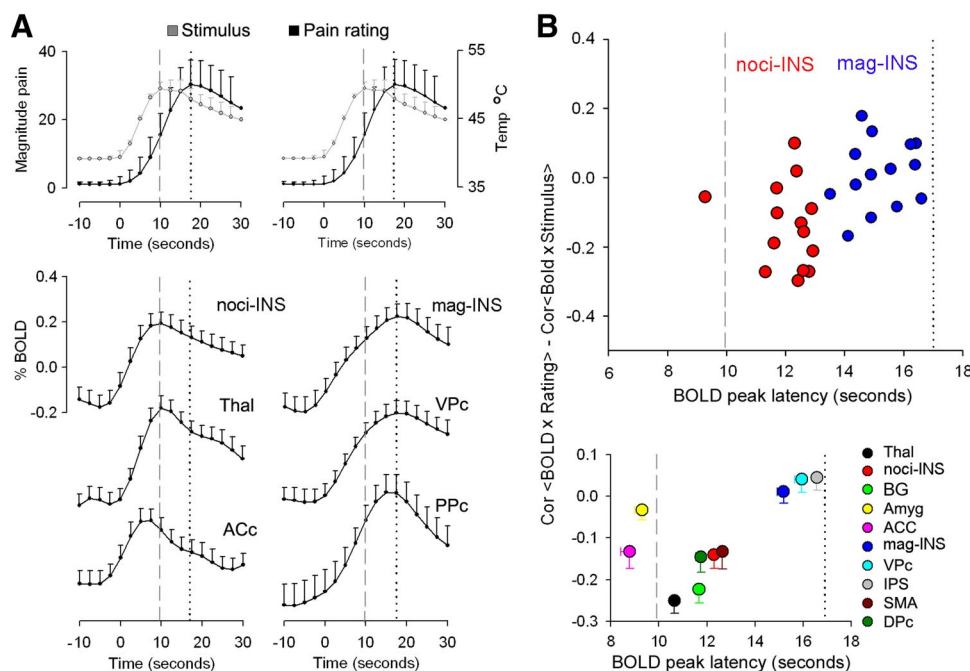

FIG. 5. Timing of BOLD signals across brain regions during pain-rating task. *A, top panels*: the average time course of the stimulus and rating (convolved with hemodynamic function, shown twice to be compared with respective time courses below). Time course of average BOLD responses (bars are SE) for pain-specific areas (*left column*) and for brain regions derived from the conjunction of variance-related maps (*right column*). The ordinates represent the average BOLD signal for each area across 110 stimulation events and the abscissa represents the time from the start of the stimulus (time = 0 s). *B, top*: the stimulus-rating indices for mag-INS and noci-INS (correlation of signal of brain region with rating − correlation with stimulus) plotted as a function of the peak response latency for each cortical area from the start of application of the stimulus in each subject. The distributions of noci-INS and mag-INS show no overlap, as indicated by color markings. The mean (and SE) for stimulus-rating indices for each area across all subjects are shown in the *bottom panel*.
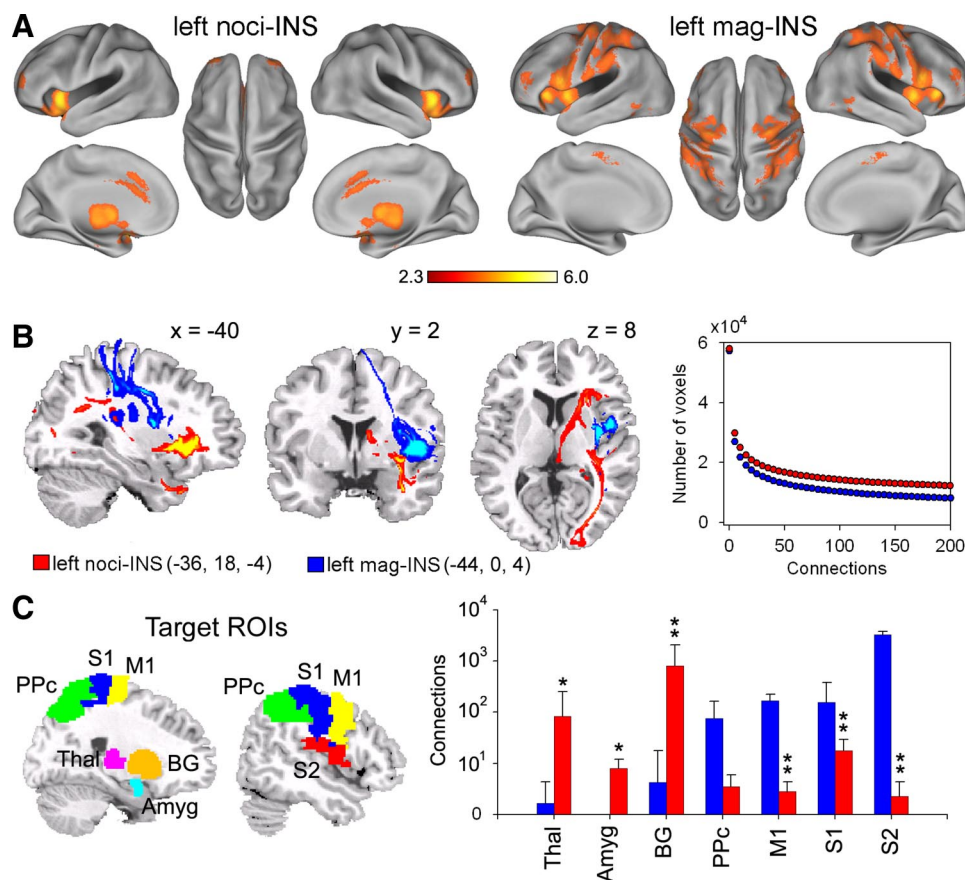
FIG. 6. Functional and anatomical dissociation in the insula. *A*: functional connectivity maps for left noci-INS and mag-INS. noci-INS exhibits strong connectivity to pain-specific regions, including bilateral thalamus, putamen, caudate, and amygdala, in addition to ACc and ventral striatum. In contrast, mag-INS shows strong connectivity to task-related regions including bilateral PPc, DPc, SMA, and lateral frontal regions. *B*: probabilistic maps of white matter tracts for left mag-INS (blue) and noci-INS (right), determined in a separate group of subjects than the subjects studied with fMRI. *Right graph* shows the number of connections averaged across all subjects as a function of threshold of connectivity. *C*: right colored brain regions illustrate the targets used in connectivity. Bar graph displays the target connectivity (examined only ipsilateral to the seed) for mag-INS and noci-INS. Consistent with the functional connectivity maps, mag-INS (blue bars) had significantly higher connections with M1, S1, and S2, whereas noci-INS (red bars) had higher connections with amygdala, thalamus, and basal ganglia. Bars are median $\pm$ quartile range. $*P < 0.01$; $**P < 0.01$.

subcortical and cortical targets. The target ROIs were defined using automated anatomical labeling based on a macroscopic anatomical parcellation of a single-subject brain (Tzourio-Mazoyer et al. 2002) and included ipsilateral amygdala, thalamus, BG, S1, M1, and PPc. The noci-INS showed significantly higher connections with subcortical regions including the thalamus, BG, and amygdala. In contrast, the mag-INS showed stronger connectivity to cortical regions, including S1, S2, and M1. Thus we observe generally similar functional and anatomical connectivity patterns and both distinguish between noci-INS and mag-INS.

DISCUSSION

The primary result of this study is the observation that brain regions that best convey properties of pain perception—i.e., mag-INS in contiguity with VPc—are areas that also represent the size of visual inputs (in this case the length of bars). As a corollary we do not observe any brain regions that uniquely relate to perceived pain. The fact that the same region captures the subjective perception of thermal painful stimulus intensities and the size of visual inputs prompts the conclusion that the region is specialized for extracting the sizes of things as an integrated concept across sensory modalities. Visual cortical areas have been reported to respond to size-related properties (Perna et al. 2005); previous evidence also shows that visual stimuli activate parts of the insula (e.g., Herdener et al. 2008) and we do not know whether magnitude is the only visual property represented in the insula. The mag-INS shares properties with the general task-related network, by *1*) reflecting

task variance, *2*) exhibiting BOLD activity delayed from the stimulus peak and just preceding pain perception peak, *3*) better correlating with the time course of pain ratings, and *4*) functionally correlating with task-activated regions. Nevertheless, this region is unique in that it shows the best relationship with both perceived pain magnitudes and perceived magnitudes for visual bars. Remarkably, the brain intrinsic functional connectivity of mag-INS essentially identifies the general task-related network and we observe that this network is grounded in anatomical connections paralleling the functional connectivity. In contrast, circumscribed cortical and subcortical areas—i.e., noci-INS, ACc, thalamus, and BG—participate in nociceptive representations and preferentially encode thermal stimulus properties; the brain intrinsic connectivity of noci-INS identifies these same regions as a functional network. The proximity of mag-INS to noci-INS suggests that this area of the insula serves as the interface between nociceptive representation and pain perception, mediated by the interaction between the two nonoverlapping networks.

To our knowledge this is the first study examining brain representation for the variance of a condition. Generally one attempts to minimize variance when exploring brain activity; as a result the variance remains within a tight range. By nature pain provides a wide range of perceived magnitudes across subjects. Here we are able to show that the variability of pain perception, the range of which spanned two folds, matches brain activity for variability of rating visual stimuli, the range of which we artificially imposed on the subjects. The brain regions identified by variance were essentially the same as those reported for task control (Dosenbach et al. 2006) and

spatial attention (Corbetta and Shulman 2002; Pihlajamaki et al. 2005). Within this group of brain areas only mag-INS and VPc coded perceived magnitudes for pain and vision equally well, for every stimulus epoch. This study is also the first to demonstrate the spatiotemporal transformation of nociceptive information in the brain. Here too the nature of pain, with its underlying nonlinear stimulus–perception transformations, aids in disentangling stimulus from perception time courses, thereby enabling the unraveling of the temporal sequence of brain activity. This analysis segregated brain regions into distinct clusters: dissociated mag-INS from noci-INS and localized noci-INS in the cluster of nociceptive representation and mag-INS in those related to task control. The third novel approach used here was the idea that given a functional segregation between two brain areas, mag-INS and noci-INS, we can test underlying anatomical segregation by transforming their coordinates to a new group of subjects and examining their respective white matter connectivities. With this approach, we observe not only connectivity differences between the two areas across the brain, but also the probabilistic connectivities that closely reflect the functional network identified in a separate group of participants based on fMRI. The latter is the first demonstration supporting the idea that anatomical and functional connectivity are tightly interrelated.

Given that all sensory modalities access the insula, we advance the notion that insular areas with properties similar to those of mag-INS should also be present for other senses as well (Augustine 1996; Cipolloni and Pandya 1999; Critchley 2005; de Araujo et al. 2003; Hanamori et al. 1998; Mesulam and Mufson 1982; Rolls 2007). It is noteworthy that taste representation in the insula is localized to a region either overlapping with or in very close proximity to mag-INS and noci-INS. Moreover, this taste region seems organized in a pattern that closely parallels the dual pain representation by mag-INS and noci-INS. An anterior taste region, dubbed "primary taste region," represents taste modalities and their intensities independent of the motivational or satiety state of the person (de Araujo et al. 2003; Rolls 2007), which matches noci-INS in both location and response properties. On the other hand, a region just posterior to this primary taste area is activated for tastes and for water in the mouth, with responses for water observed only when subjects are thirsty (de Araujo et al. 2003). The latter corresponds to mag-INS both in location and response property because it reflects perceived magnitude for tastants rather than for stimulus intensity. These similarities suggest that taste and pain parallel each other in organization in the insula and imply that a similar organization may also exist for other senses, which needs to be systematically explored. The close spatial proximity of taste and pain representation, wherein visual magnitudes are also represented, raises the question as to the extent to which these modalities converge on the same neurons. Single-unit electrophysiological studies in the rat insula indicate that individual neurons can respond convergently to painful pinch, gustatory, and visceral inputs (Hanamori et al. 1998). There are similar reports in nonhuman primates as well. Whether individual neurons would respond to visual and painful inputs remains unknown, but is suggested both by our results and by the existing single-neuron studies.

There is extensive evidence implicating the involvement of the insula in pain perception. Here we extend this idea by differentiating between stimulus encoding and the subjectively perceived magnitude of pain. A number of recent studies show a remarkable overlap between brain regions underlying the assessment of painful stimulation in the self and in others (empathy for pain), involving common activity in bilateral insula and mACc (Jackson et al. 2005; Singer et al. 2004). Not only the presence of pain but also the intensity of others' pain seems to be captured by these regions (Jackson et al. 2005). This overlap in activity has been attributed to "mirroring" the affective dimension of pain. We propose a more parsimonious explanation: that sensory input is integrated and encoded within the insula (Burton and Sinclair 2000) to generate a magnitude estimation signal even in the case of empathy. Along these lines, our results suggest that insular lesions affecting pain perception (Berthier et al. 1988; Schmahmann and Leifer 1992) may be a consequence of multiple abnormalities, depending on the location and extent of the lesion: reduced ability in either nociceptive representation (if the lesion mainly influences noci-INS), or in magnitude perception more generally (if mag-INS is injured), or some combination of both, which would become apparent if such patients' abilities of rating other sensory magnitudes were tested. Indeed, recent studies show that insular lesions lead to cessation of addictive smoking behavior (Naqvi et al. 2007) and abnormal risk assessment (Clark et al. 2008). Our results suggest that these may be a consequence of a diminished ability to gauge perceived magnitudes for reward and risk. The insular cortex has been shown to be activated for all sensory modalities and implicated in a very large number of seemingly unrelated tasks (>23,000 citations are identified in Pubmed for the search term "functional MRI and pain"), although a review of these studies is beyond the scope of this study. The present results suggest that many of these studies may be recast from the viewpoint that subjective magnitude estimation may be a contributing parameter, which in turn provides a unifying idea for the role of the insula in the myriad of tasks in which it has been implicated.

There is emerging evidence demonstrating frontal and parietal regions as integral to the formation of subjective perception and experience from incoming sensory stimuli (de Lafuente and Romo 2006). The present study identified a similar cortical network underlying pain and visual rating that included bilateral insula, posterior parietal cortex, ventral and dorsal portions of the premotor cortex, and supplementary motor area and this activity pattern closely matches brain areas identified in a tactile-discrimination task (Pleger et al. 2006), which outside of the stimulus-specific activations seem essentially identical to the task-related network we observed for both visual- and pain-rating tasks. Importantly, our results show that activity of these brain regions was associated with the amount of information of the subjective perception reported. Consistent with our results, these areas play a role in number representation in humans (Piazza et al. 2007) and in encoding the subjective sensory experiences in monkeys (de Lafuente and Romo 2006). It is important to note that only selective regions within this network, i.e., the mag-INS and VPc, encoded magnitude of perception.

Caveats

The linear stimulus–perception transformation for visual magnitudes limits our ability in studying the information trans-

formation that may underlie visually driven activity observed in mag-INS. Future studies are required where one can examine brain activity differences for identifying objects and their spatial locations, when they are matched in size, and contrast them when the size parameter is varied. Moreover, we extrapolate from present results that general magnitude assessment is likely being extracted in mag-INS. This necessitates future studies where perceived magnitude for touch, sound, smell, and taste are also systematically studied.

Conclusions

Overall, we conclude that, analogous and in addition to the "what" and "where" of functional networks associated with the ventral and dorsal visual pathways (Goodale and Milner 1992; Ungerleider and Haxby 1994), there also exists a central module for sensory "how much," localized to the insula and extending into the lateral prefrontal cortex. The saliency of painful stimuli necessitates the activation of this "how much" system even when subjects are instructed not to attend to the pain and the transfer of nociceptive information from other brain regions to the "how much" system gives rise to a subjective percept of pain. Prior to this work, a general central mechanism for magnitude perception has been theorized but never demonstrated (Walsh 2003). It is remarkable that the properties of the "how much" module we have identified in this study—its extensive connectivity, particularly to the posterior parietal cortex, and its location extending from the insula to the lateral prefrontal cortex—all correspond to the anterior portion of this theorized magnitude network.

REFERENCES

Alexander AL, Lee JE, Lazar M, Field AS. Diffusion tensor imaging of the brain. *Neurotherapeutics* 4: 316–329, 2007.

Apkarian AV, Bushnell MC, Treede RD, Zubieta JK. Human brain mechanisms of pain perception and regulation in health and disease. *Eur J Pain* 9: 463–484, 2005.

Apkarian AV, Darbar A, Krauss BR, Gelnar PA, Szeverenyi NM. Differentiating cortical areas related to pain perception from stimulus identification: temporal analysis of fMRI activity. *J Neurophysiol* 81: 2956–2963, 1999.

Apkarian AV, Krauss BR, Fredrickson BE, Szeverenyi NM. Imaging the pain of low back pain: functional magnetic resonance imaging in combination with monitoring subjective pain perception allows the study of clinical pain states. *Neurosci Lett* 299: 57–60, 2001.

Augustine JR. Circuitry and functional aspects of the insular lobe in primates including humans. *Brain Res Brain Res Rev* 22: 229–244, 1996.

Baliki MN, Chialvo DR, Geha PY, Levy RM, Harden RN, Parrish TB, Apkarian AV. Chronic pain and the emotional brain: specific brain activity associated with spontaneous fluctuations of intensity of chronic back pain. *J Neurosci* 26: 12165–12173, 2006.

Baliki MN, Geha PY, Apkarian AV, Chialvo DR. Beyond feeling: chronic pain hurts the brain, disrupting the default-mode network dynamics. *J Neurosci* 28: 1398–1403, 2008.

Beaulieu C. The basis of anisotropic water diffusion in the nervous system: a technical review. *NMR Biomed* 15: 435–455, 2002.

Behrens TE, Johansen-Berg H, Woolrich MW, Smith SM, Wheeler-Kingshott CA, Boulby PA, Barker GJ, Sillery EL, Sheehan K, Ciccarelli O, Thompson AJ, Brady JM, Matthews PM. Non-invasive mapping of connections between human thalamus and cortex using diffusion imaging. *Nat Neurosci* 6: 750–757, 2003a.

Behrens TE, Woolrich MW, Jenkinson M, Johansen-Berg H, Nunes RG, Clare S, Matthews PM, Brady JM, Smith SM. Characterization and propagation of uncertainty in diffusion-weighted MR imaging. *Magn Reson Med* 50: 1077–1088, 2003b.

Berthier M, Starkstein S, Leiguarda R. Asymbolia for pain: a sensory-limbic disconnection syndrome. *Ann Neurol* 24: 41–49, 1988.

Buchel C, Bornhovd K, Quante M, Glauche V, Bromm B, Weiller C. Dissociable neural responses related to pain intensity, stimulus intensity, and stimulus awareness within the anterior cingulate cortex: a parametric single-trial laser functional magnetic resonance imaging study. *J Neurosci* 22: 970–976, 2002.

Burton H, Sinclair RJ. Attending to and remembering tactile stimuli: a review of brain imaging data and single-neuron responses. *J Clin Neurophysiol* 17: 575–591, 2000.

Cipolloni PB, Pandya DN. Cortical connections of the frontoparietal opercular areas in the rhesus monkey. *J Comp Neurol* 403: 431–458, 1999.

Clark L, Bechara A, Damasio H, Aitken MR, Sahakian BJ, Robbins TW. Differential effects of insular and ventromedial prefrontal cortex lesions on risky decision-making. *Brain* 131: 1311–1322, 2008.

Coghill RC, Sang CN, Maisog JM, Iadarola MJ. Pain intensity processing within the human brain: a bilateral, distributed mechanism. *J Neurophysiol* 82: 1934–1943, 1999.

Corbetta M, Shulman GL. Control of goal-directed and stimulus-driven attention in the brain. *Nat Rev Neurosci* 3: 201–215, 2002.

Cowan N. The magical number 4 in short-term memory: a reconsideration of mental storage capacity. *Behav Brain Sci* 24: 87–114, 2001.

Critchley HD. Neural mechanisms of autonomic, affective, and cognitive integration. *J Comp Neurol* 493: 154–166, 2005.

de Araujo IE, Kringelbach ML, Rolls ET, McGlone F. Human cortical responses to water in the mouth, and the effects of thirst. *J Neurophysiol* 90: 1865–1876, 2003.

de Lafuente V, Romo R. Neural correlate of subjective sensory experience gradually builds up across cortical areas. *Proc Natl Acad Sci USA* 103: 14266–14271, 2006.

Derbyshire SW, Jones AK, Gyulai F, Clark S, Townsend D, Firestone LL. Pain processing during three levels of noxious stimulation produces differential patterns of central activity. *Pain* 73: 431–445, 1997.

Dosenbach NU, Visscher KM, Palmer ED, Miezin FM, Wenger KK, Kang HC, Burgund ED, Grimes AL, Schlaggar BL, Petersen SE. A core system for the implementation of task sets. *Neuron* 50: 799–812, 2006.

Fechner GT. *Elemente der psychophysik* (*Vol. 1*) [*Elements of Psychophysics* (*Vol. 1*)], translated by Adler HE and edited by Howes DH, Boring EG. New York: Holt, Rinehart & Winston, 1966 (original work published in 1860).

Fox MD, Snyder AZ, Vincent JL, Corbetta M, Van Essen DC, Raichle ME. The human brain is intrinsically organized into dynamic, anticorrelated functional networks. *Proc Natl Acad Sci USA* 102: 9673–9678, 2005.

Friston KJ, Holmes AP, Worsley KJ, Poline J-B, Frith CD, Frackowiak RS. Statistic parametric maps in functional imaging: a general linear approach. *Hum Brain Mapp* 2: 189–210, 1995.

Fulbright RK, Manson SC, Skudlarski P, Lacadie CM, Gore JC. Quantity determination and the distance effect with letters, numbers, and shapes: a functional MR imaging study of number processing. *Am J Neuroradiol* 24: 193–200, 2003.

Geha PY, Baliki MN, Harden RN, Bauer WR, Parrish TB, Apkarian AV. The brain in chronic CRPS pain: abnormal gray-white matter interactions in emotional and autonomic regions. *Neuron* 60: 570–581, 2008.

Gescheider GA. Psychophysical measurement of thresholds: differential sensitivity. In: *Psychophysics: The Fundamentals*. Hillsdale, NJ: Erlbaum, 1997, p. 1–15.

Giesecke T, Gracely RH, Grant MA, Nachemson A, Petzke F, Williams DA, Clauw DJ. Evidence of augmented central pain processing in idiopathic chronic low back pain. *Arthritis Rheum* 50: 613–623, 2004.

Gobel SM, Johansen-Berg H, Behrens T, Rushworth MF. Response-selection-related parietal activation during number comparison. *J Cogn Neurosci* 16: 1536–1551, 2004.

Goodale MA, Milner AD. Separate visual pathways for perception and action. *Trends Neurosci* 15: 20–25, 1992.

Hanamori T, Kunitake T, Kato K, Kannan H. Responses of neurons in the insular cortex to gustatory, visceral, and nociceptive stimuli in rats. *J Neurophysiol* 79: 2535–2545, 1998.

Herdener M, Lehmann C, Esposito F, di Salle F, Federspiel A, Bach DR, Scheffler K, Seifritz E. Brain responses to auditory and visual stimulus offset: shared representations of temporal edges. *Hum Brain Mapp* (February 11, 2008). [Epub ahead of print].

Jackson PL, Meltzoff AN, Decety J. How do we perceive the pain of others? A window into the neural processes involved in empathy. *Neuroimage* 24: 771–779, 2005.

Kong J, White NS, Kwong KK, Vangel MG, Rosman IS, Gracely RH, Gollub RL. Using fMRI to dissociate sensory encoding from cognitive evaluation of heat pain intensity. *Hum Brain Mapp* 27: 715–721, 2006.

Kwan CL, Diamant NE, Pope G, Mikula K, Mikulis DJ, Davis KD. Abnormal forebrain activity in functional bowel disorder patients with chronic pain. *Neurology* 65: 1268–1277, 2005.

Lorenz J, Cross DJ, Minoshima S, Morrow TJ, Paulson PE, Casey KL. A unique representation of heat allodynia in the human brain. *Neuron* 35: 383–393, 2002.

Melzack R, Katz J. Pain measurements in persons with pain. In: *Textbook of Pain*, edited by Wall PD, Melzack R. London: Churchill Livingstone, 1999, p. 409–426.

Mesulam MM, Mufson EJ. Insula of the old world monkey. I. Architectonics in the insulo-orbito-temporal component of the paralimbic brain. *J Comp Neurol* 212: 1–22, 1982.

Miller GA. The magical number seven, plus or minus two: some limits on our capacity for processing information. *Psychol Rev* 63: 81–97, 1956.

Naqvi NH, Rudrauf D, Damasio H, Bechara A. Damage to the insula disrupts addiction to cigarette smoking. *Science* 315: 531–534, 2007.

Nielsen CS, Price DD, Vassend O, Stubhaug A, Harris JR. Characterizing individual differences in heat-pain sensitivity. *Pain* 119: 65–74, 2005.

Perna A, Tosetti M, Montanaro D, Morrone MC. Neuronal mechanisms for illusory brightness perception in humans. *Neuron* 47: 645–651, 2005.

Piazza M, Pinel P, Le Bihan D, Dehaene S. A magnitude code common to numerosities and number symbols in human intraparietal cortex. *Neuron* 53: 293–305, 2007.

Pihlajamaki M, Tanila H, Kononen M, Hanninen T, Aronen HJ, Soininen H. Distinct and overlapping fMRI activation networks for processing of novel identities and locations of objects. *Eur J Neurosci* 22: 2095–2105, 2005.

Pleger B, Ruff CC, Blankenburg F, Bestmann S, Wiech K, Stephan KE, Capilla A, Friston KJ, Dolan RJ. Neural coding of tactile decisions in the human prefrontal cortex. *J Neurosci* 26: 12596–12601, 2006.

Price DD. *Psychological and Neural Mechanisms of Pain.* New York: Raven Press, 1988.

Price DD. Psychological and neural mechanisms of the affective dimension of pain. *Science* 288: 1769–1772, 2000.

Rainville P, Duncan GH, Price DD, Carrier B, Bushnell MC. Pain affect encoded in human anterior cingulate but not somatosensory cortex. *Science* 277: 968–971, 1997.

Rolls ET. Sensory processing in the brain related to the control of food intake. *Proc Nutr Soc* 66: 96–112, 2007.

Schmahmann JD, Leifer D. Parietal pseudothalamic pain syndrome. Clinical features and anatomic correlates. *Arch Neurol* 49: 1032–1037, 1992.

Schoedel AL, Zimmermann K, Handwerker HO, Forster C. The influence of simultaneous ratings on cortical BOLD effects during painful and non-painful stimulation. *Pain* 135: 131–141, 2008.

Shannon CE, Weaver W. *The Mathematical Theory of Communication.* Urbana, IL: Univ. of Illinois Press, 1949.

Singer T, Seymour B, O'Doherty J, Kaube H, Dolan RJ, Frith CD. Empathy for pain involves the affective but not sensory components of pain. *Science* 303: 1157–1162, 2004.

Smith SM, Jenkinson M, Woolrich MW, Beckmann CF, Behrens TE, Johansen-Berg H, Bannister P, De Luca CJ, Drobnjak I, Flitney DE, Nianzy R, Saunders J, Vickers J, Zhang Y, De Stefano N, Brady JM, Mathews PM. Advances in functional and structural MR image analysis and implementation as FSL. *Neuroimage* 23, *Suppl.* 1: 208–219, 2004.

Stevens SS. On the psychophysical law. *Psychol Rev* 64: 153–181, 1957.

Teghtsoonian R. On the exponents in Stevens' law and the constant in Ekman's law. *Psychol Rev* 78: 71–80, 1971.

Tzourio-Mazoyer N, Landeau B, Papathanassiou D, Crivello F, Etard O, Delcroix N, Mazoyer B, Joliot M. Automated anatomical labeling of activations in SPM using a macroscopic anatomical parcellation of the MNI MRI single-subject brain. *Neuroimage* 15: 273–289, 2002.

Ungerleider LG, Haxby JV. "What" and "where" in the human brain. *Curr Opin Neurobiol* 4: 157–165, 1994.

Van Essen DC. A Population-Average, Landmark- and Surface-based (PALS) atlas of human cerebral cortex. *Neuroimage* 28: 635–662, 2005.

Walsh V. A theory of magnitude: common cortical metrics of time, space and quantity. *Trends Cogn Sci* 7: 483–488, 2003.

Weber EH. *The Sense of Touch*, translated by Ross HE, Murray DJ. London: Academic Press, 1978 (original work published in 1834).

Woolrich MW, Behrens TE, Beckmann CF, Jenkinson M, Smith SM. Multilevel linear modelling for FMRI group analysis using Bayesian inference. *Neuroimage* 21: 1732–1747, 2004.

Woolrich MW, Ripley BD, Brady M, Smith SM. Temporal autocorrelation in univariate linear modeling of FMRI data. *Neuroimage* 14: 1370–1386, 2001.